CrossMark

First Passage Time for Brownian Motion and Piecewise Linear Boundaries

Zhiyong Jin[1] · Liqun Wang[1,2]

Abstract We propose a new approach to calculating the first passage time densities for Brownian motion crossing piecewise linear boundaries which can be discontinuous. Using this approach we obtain explicit formulas for the first passage densities and show that they are continuously differentiable except at the break points of the boundaries. Furthermore, these formulas can be used to approximate the first passage time distributions for general nonlinear boundaries. The numerical computation can be easily done by using the Monte Carlo integration, which is straightforward to implement. Some numerical examples are presented for illustration. This approach can be further extended to compute two-sided boundary crossing distributions.

Keywords Boundary crossing density · Brownian motion · First hitting time · First passage time · Curved boundary

Mathematics Subject Classification (2010) Primary 60J65, 60J75 · Secondary 60J60, 60J70

1 Introduction

Let $W = \{W_t, t \geq 0\}$ be a standard Brownian motion starting at $W_0 = 0$ and $c(t), t \geq 0$ be a real function with $c(0) > 0$. The first passage time (FPT) of W with respect to c is defined as

$$\tau_c = \inf\{t > 0 : W_t \geq c(t)\}, \tag{1}$$

✉ Liqun Wang
liqun.wang@umanitoba.ca

[1] Department of Statistics, University of Manitoba, Winnipeg, Manitoba R3T 2N2, Canada

[2] School of Science, Beijing Jiaotong University, Beijing, China

 Springer

and the corresponding boundary non-crossing probability (BNCP) at any $t > 0$ is

$$P(t; c) = P(\tau_c > t) = P(W_s < c(s), \forall s \in [0, t]). \tag{2}$$

Then the first passage density (FPD) of W at $t > 0$ is the rate of decrease of $P(t; c)$ and, if exists, is given by

$$f_c(t) = -\frac{\mathrm{d}P(t; c)}{\mathrm{d}t}. \tag{3}$$

The first passage time plays an important role in stochastic modelling in many scientific disciplines, including biology, chemistry, physics, environmental science, engineering, epidemiology, as well as in finance, economics, and business and management. However, the calculation of the FPT distributions is difficult in general and has been the subject of research for many decades. Explicit formulas exist only in a few special cases, such as for Brownian motion and linear boundaries. For example, for a linear boundary $c(t) = at + b$ with $b > 0$, the BNCP and FPD have simple closed-form expressions

$$P(t; c) = \Phi\left(\frac{at + b}{\sqrt{t}}\right) - \exp(-2ab)\Phi\left(\frac{at - b}{\sqrt{t}}\right) \tag{4}$$

and

$$f_c(t) = \frac{b}{\sqrt{2\pi t^3}} \exp\left[-\frac{(at + b)^2}{2t}\right], \tag{5}$$

where $\Phi(\cdot)$ is the standard Gaussian distribution function (Karatzas and Shreve 1991).

For Brownian motion and more general boundaries various methods have been used to find numerical approximations of the FPT densities, such as tangent approximation (Strassen 1967; Ferebee 1982; Lerche 1986), method of images (Daniels 1982; 1996), and series expansions (Durbin 1971; Ferebee 1983; Durbin and Williams 1992). Some other researchers use Volterra integral equations to approximate the FPD for more general diffusion processes (Ricciardi et al. 1984; Buonocore et al. 1987; Lehmann 2002). More recently, Taillefumier and Magnasco (Taillefumier and Magnasco 2010) proposed a discrete simulation-based algorithm to approximate the FPD of Gauss-Markov processes and Hölder continuous boundaries, while Molini et al. (Molini et al. 2011) obtained the approximation by solving a Fokker-Planck equation subject to an absorbing boundary and deriving the transition probability using the method of image. Besides heavy computational cost, all these methods apply to continuous or differentiable boundaries only.

In this paper, we propose a different approach that is applicable for discontinuous as well as continuous boundaries. Using this approach we derive a formula for the FPT density for Brownian motion crossing a piecewise linear boundary. We show that the density is differentiable everywhere except possibly at the break points of the boundary. Moreover, we use this formula to approximate the FPT density for more general nonlinear smooth boundaries. Numerical computation can be done by Monte Carlo integration method which is straightforward and easy to implement. The numerical examples show that fairly good approximation results can be obtained with moderate computational burden. This approach is based on the method of iterative expectation of Wang and Pötzelberger (Wang and Pötzelberger 1997) that combines the total probability and Markov property of the Brownian motion.

The rest of the paper is organized as follows. In Sections 2 and 3 we derive the explicit formulas of the BCP and FPD for Brownian motion and piecewise linear boundaries. These formulas are used to approximate the BCP and FPD for general boundaries

in Section 4. The BCP and FPD for more general diffusion processes which can be expressed as functionals of a standard Brownian motion are considered in Section 5, while numerical computation and examples are presented in Section 6. Finally conclusions and discussion are given in Section 7.

2 BCP for Piecewise Linear Boundary

In this section we first derive an explicit formula for the BCP and piecewise linear boundaries. Specifically, for any $t > 0$, let $0 = t_0 < t_1 < \cdots < t_n = t$ be a partition of $[0, t]$ and $c(s)$, $s \geq 0$ be a linear function on each interval $[t_{i-1}, t_i]$ and satisfy $\lim_{s \to 0+} c(s) = c(0) > 0$. Further, denote $c_i^+ = \lim_{s \to 0+} c(t_i + s)$, $c_i^- = \lim_{s \to 0+} c(t_i - s)$, $c_i = \min\{c_i^+, c_i^-\}$, $c_0 = c_0^+ = c(0)$ and $c_n = c_n^- = c(t)$. So the boundary can be discontinuous at some t_i.

Theorem 1 *For any $t > 0$ and piecewise linear boundary $c(s)$ defined on the partition $(t_i)_{i=1}^n$ of $[0, t]$, the BNCP is given by*

$$P(t; c) = E g_n(W_{t_1}, W_{t_2}, \ldots, W_{t_n}; c), \tag{6}$$

where

$$g_n(\boldsymbol{x}; c) = \prod_{i=1}^n \mathbb{1}\{x_i < c_i\} \left\{ 1 - \exp\left[- \frac{2(c_{i-1}^+ - x_{i-1})(c_i^- - x_i)}{t_i - t_{i-1}} \right] \right\} \tag{7}$$

and $\boldsymbol{x} = (x_1, x_2, \cdots, x_n)$, $x_0 = 0$ and $\mathbb{1}\{\cdot\}$ is the indicator function.

Proof By the Markov property of Brownian motion, we have

$$
\begin{aligned}
P(t; c) &= P(W_s < c(s), 0 \leq s \leq t) \\
&= E P(W_s < c(s), \forall s \in \bigcup_{i=1}^n (t_{i-1}, t_i) | W_{t_1}, W_{t_2}, \ldots, W_{t_n}) \\
&= E \prod_{i=1}^n P(W_s < c(s), t_{i-1} < s < t_i | W_{t_{i-1}}, W_{t_i}).
\end{aligned}
$$

The result follows then from

$$
\begin{aligned}
P(W_s &< c(s), t_{i-1} < s < t_i | W_{t_{i-1}} = x_{i-1}, W_{t_i} = x_i) \\
&= P(W_s < c(s + t_{i-1}) - x_{i-1}, 0 < s < t_i - t_{i-1} | W_{t_i - t_{i-1}} = x_i - x_{i-1}) \\
&= \mathbb{1}\{x_{i-1} < c_{i-1}^+\} \mathbb{1}\{x_i < c_i^-\} \left\{ 1 - \exp\left[- \frac{2(c_{i-1}^+ - x_{i-1})(c_i^- - x_i)}{t_i - t_{i-1}} \right] \right\},
\end{aligned}
$$

where the last equality follows from the well-known formula of the conditional crossing probability (Siegmund 1986). □

When $c(t)$ is continuous on $[0, t]$, we have $c_i = c_i^+ = c_i^- = c(t_i)$, $i = 1, 2, \ldots, n$, and Eq. 6 reduces to the formula of Wang and Pötzelberger (Wang and Pötzelberger 1997) who obtained the result by using the iterative integration. Here, we give an alternative form of this formula which is obtained by a simple change of variable in the integration.

Corollary 2 *For any $t > 0$ and continuous piecewise linear boundary $c(s)$ defined on the partition $(t_i)_{i=1}^n$ of $[0, t]$, the BNCP is given by*

$$P(t; c) = E g_n(W_{t_1} - c_1, W_{t_2} - c_2, \ldots, W_{t_n} - c_n), \tag{8}$$

where

$$g_n(\boldsymbol{x}) = \mathbb{1}\{\boldsymbol{x} \in \mathbb{R}_+^n\} \prod_{i=1}^{n} [1 - \exp\left(-\frac{2x_{i-1}x_i}{t_i - t_{i-1}}\right)], \tag{9}$$

$x_0 = c_0$ and $\mathbb{R}_+^n = (0, \infty)^n$.

3 FPD for Piecewise Linear Boundary

Now we consider the FPT density for a piecewise linear boundary. Let $0 = t_0 < t_1 < \cdots < t_n < \cdots$ be a partition of $[0, \infty)$ such that $\lim_{n \to \infty} t_n = \infty$. Again let $c(t), t \geq 0$ be a linear function on each interval $[t_{i-1}, t_i]$ and satisfy $\lim_{t \to 0+} c(t) = c(0) > 0$. Further, let c_i, c_i^+, c_i^- be defined as before. Then we have the following result.

Theorem 3 *For any piecewise linear boundary $c(t)$ defined on the partition $(t_i)_{i=1}^\infty$, the FPD of W at any $t \in (t_{n-1}, t_n)$ is given by*

$$f(t; c) = E h_{n-1}(W_{t_1}, W_{t_2}, \ldots, W_{t_{n-1}}; c), \tag{10}$$

where

$$h_{n-1}(\boldsymbol{x}; c) = g_{n-1}(\boldsymbol{x}; c)\phi(t - t_{n-1}, x_{n-1}, c(t)) \frac{c_{n-1}^+ - x_{n-1}}{t - t_{n-1}} \tag{11}$$

and

$$\phi(t - s, x, y) = \frac{1}{\sqrt{2\pi(t - s)}} \exp\left[-\frac{(y - x)^2}{2(t - s)}\right] \tag{12}$$

is the transition density of W from (s, x) to (t, y). Furthermore, $f(t; c)$ is continuously differentiable at t.

Proof Let

$$f_n(\boldsymbol{x}) = \prod_{i=1}^{n} \frac{1}{\sqrt{2\pi(t_i - t_{i-1})}} \exp\left[-\frac{(x_i - x_{i-1})^2}{2(t_i - t_{i-1})}\right]$$

be the joint pdf of $(W_{t_1}, W_{t_2}, \ldots, W_{t_n})$. Then we can write the expectation Eq. 6 as

$$P(t; c) = \int \prod_{i=1}^{n} \mathbb{1}\{x_i < c_i\} \left\{ 1 - \exp\left[-\frac{2(c_{i-1}^+ - x_{i-1})(c_i^- - x_i)}{t_i - t_{i-1}}\right] \right\} f_n(\boldsymbol{x}) \mathrm{d}\boldsymbol{x}$$

$$= \int_{-\infty}^{c(t)} p(t, x) \mathrm{d}x, \tag{13}$$

where

$$p(t, x) = \int q(t, x) g_{n-1}(\boldsymbol{x}; c) f_{n-1}(\boldsymbol{x}) \mathrm{d}\boldsymbol{x}$$

with

$$q(t, x) = \frac{1}{\sqrt{2\pi(t - t_{n-1})}} \exp[-\frac{(x - x_{n-1})^2}{2(t - t_{n-1})}]\left\{1 - \exp\left[-\frac{2(c_{n-1}^+ - x_{n-1})(c(t) - x)}{t - t_{n-1}}\right]\right\}.$$

Now we show that function $p(t, x)$ satisfies the following diffusion equation (also called Fokker-Planck or Kolmogorov equation)

$$\frac{\partial p(t, x)}{\partial t} = \frac{1}{2}\frac{\partial^2 p(t, x)}{\partial x^2}. \tag{14}$$

To this end it suffices to show that $q(t, x)$ satisfies the above equation because it is the only part of $p(t, x)$ that depends on (t, x). This can be verified by noting that $q(t, x)$ can be written as

$$q(t, x) = \phi(t - t_{n-1}, x_{n-1}, x) - \phi(t - t_{n-1}, 2c_{n-1} - x_{n-1}, x) \exp[-2c'(t)(c_{n-1} - x_{n-1})]$$

where the Gauss kernel $\phi(t - s, y, x)$ is well-known to satisfy Eq. 14 and $c'(t)$ is a constant that is the slope of the piecewise linear boundary on interval (t_{n-1}, t). Further, since $p(t, c(t)) = 0$, it follows from Eqs. 13 and 14 that

$$\begin{aligned}
\frac{\partial P(t; c)}{\partial t} &= \int_{-\infty}^{c(t)} \frac{\partial p(t, x)}{\partial t} dx \\
&= \frac{1}{2} \int_{-\infty}^{c(t)} \frac{\partial^2 p(t, x)}{\partial x^2} dx \\
&= \frac{1}{2} \frac{\partial p(t, x)}{\partial x}\Big|_{x \uparrow c(t)}.
\end{aligned}$$

Therefore Eq. 10 follows from

$$\frac{\partial q(t, x)}{\partial x}\Big|_{x \uparrow c(t)} = -\frac{2(c_{n-1}^+ - x_{n-1})}{\sqrt{2\pi(t - t_{n-1})^3}} \exp\left[-\frac{(c(t) - x_{n-1})^2}{2(t - t_{n-1})}\right]$$

and

$$f(t; c) = -\frac{\partial P(t; c)}{\partial t} = -\frac{1}{2}\frac{\partial p(t, x)}{\partial x}\Big|_{x \uparrow c(t)}.$$

Furthermore, it is clear that $f(t; c)$ is continuously differentiable at t.   □

Similar to the BCP, for a continuous piecewise linear boundary where $c_i = c_i^+ = c_i^- = c(t_i)$, we have an alternative formula for the FPD.

Corollary 4 *For any $t \in (t_{n-1}, t_n)$, if the piecewise linear boundary $c(s)$ in Theorem 3 is continuous on $[0, t]$, then the FPD is given by*

$$f(t; c) = Eh_{n-1}(W_{t_1} - c_1, W_{t_2} - c_2, \ldots, W_{t_{n-1}} - c_{n-1}), \tag{15}$$

where

$$h_{n-1}(\boldsymbol{x}) = \frac{g_{n-1}(\boldsymbol{x})x_{n-1}}{t - t_{n-1}}\phi(t - t_{n-1}, c_{n-1} - x_{n-1}, c(t)). \tag{16}$$

From formula (10) we can see that the FPD for piecewise linear boundaries has the following interesting monotone property (Fig 1).

Corollary 5 *Let $b(s)$ and $c(s)$ be two piecewise linear boundaries such that $b(t) = c(t)$, $b(s) \leq c(s)$, $\forall s \in [0, t]$ and $b(s) < c(s)$ for some $s \in (0, t)$. Then the FPD for $b(s)$ and $c(s)$ satisfy $f(t; b) < f(t; c)$.*

Proof From Eqs. 7 and 11 we can see that $g_{n-1}(\boldsymbol{x}; c)$ and $h_{n-1}(\boldsymbol{x}; c)$ are monotone increasing functions of $c_i^+, c_i^-, i = 1, 2, \ldots, n$. Therefore $f(t; b) < f(t; c)$ if $b(s)$ and $c(s)$ are defined on the same set of partition of $[0, t]$. However, if they are defined on two different partitions, then we can merge the two sets of partition points and redefine the two boundaries on the common partition. Apparently this will not change the monotone relation between the two boundaries and their FPD values at t. Therefore we have $f(t; b) < f(t; c)$. $\square$

The result of Corollary 5 is interesting and somewhat unexpected. While it is easy to see the monotonicity property of the boundary crossing probability with respect to the boundary, this is less obvious with boundary crossing density. Moreover, while the boundary crossing probability is lower for the higher boundary, it is opposite for the density. In the following we give an example to further illustrate this point.

Example 1 Let $0 < T_1 < t$ be fixed and define $c(s) = a\mathbb{1}\{0 \leq s \leq T_1\} + c\mathbb{1}\{s > T_1\}$ and $b(s) = b\mathbb{1}\{0 \leq s \leq T_1\} + c\mathbb{1}\{s > T_1\}$, where $a > b > c > 0$ (Fig. 2). Then for any $t > T_1$,

$$P(W_s < c(s), 0 \leq s \leq t)$$
$$= \int_{-\infty}^{c} P(W_s < a, 0 \leq t \leq T_1 | W_{T_1} = x) P(W_s < c - x, 0 < s \leq t - T_1) dx.$$

and therefore

$$f(t; c) = -\frac{\partial}{\partial t} P(W_s < c(s), 0 \leq s \leq t))$$
$$= -\int_{-\infty}^{c} P(W_s < a, 0 \leq s \leq T_1 | W_{T_1} = x) \frac{\partial}{\partial t} P(W_s < c - x, 0 < s \leq t - T_1) dx.$$

Similarly, for $t > T_1$,

$$f(t; b) = -\frac{\partial}{\partial t} P(W_s < b(s), 0 \leq s \leq t))$$
$$= -\int_{-\infty}^{c} P(W_s < b, 0 \leq s \leq T_1 | W_{T_1} = x) \frac{\partial}{\partial t} P(W_s < c - x, 0 < s \leq t - T_1) dx.$$
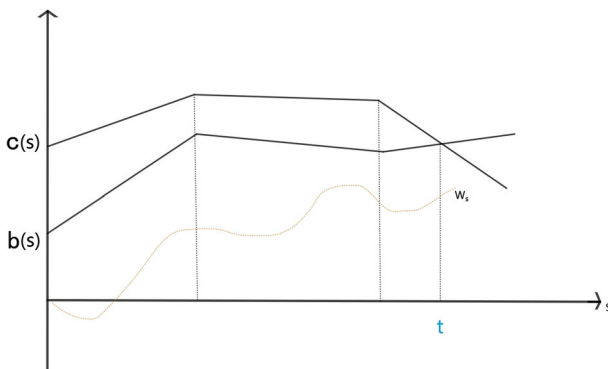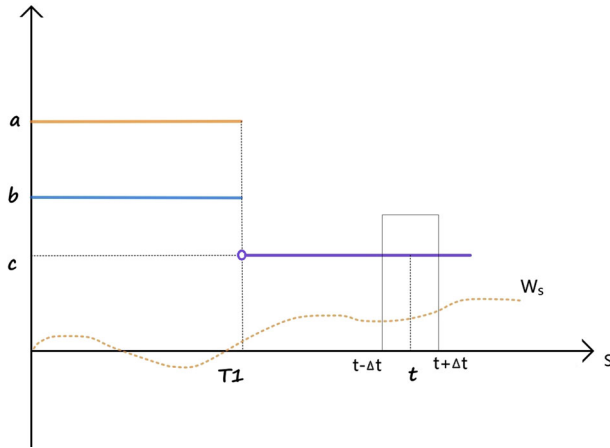

Fig. 1 Boundaries in Corollary 5

Fig. 2 Boundaries in Example 1

Since for any $x < c$,

$$P(W_s < b, 0 \le t \le T_1 | W_{T_1} = x) < P(W_s < a, 0 \le s \le T_1 | W_{T_1} = x),$$

it follows that $f(t; b) < f(t; c)$.

Now we give an experimental explanation using the example of R. Brown in 1827 who observed N pollen particles under a microscope. The displacement of each particle along a fixed axis can be regarded as a standard Brownian motion. Let $0 < T_1 < t$ be fixed. If a particle does not reach $c(s) = c$ before T_1, then it is said to be in class 1. If a particle does not reach $b(s) = b$ before T_1, then it belongs to class 2. If, after T_1, a particle reaches c in a small interval $(t - \frac{1}{2}\Delta t, t + \frac{1}{2}\Delta t)$, then it is said to be in class A. Then for sufficiently large N and small Δt, N_1/N and N_2/N can be regarded as the approximate FPD values under upper and lower boundaries respectively. It is clear that the number N_1 of particles in both class 1 and A is greater than or equal to the number N_2 of particles in both class 2 and A, that is, $N_1/N \ge N_2/N$.

4 General Nonlinear Boundaries

In this section we obtain approximations of the BCP and FPD for general nonlinear boundaries using the corresponding formulas for piecewise linear boundaries derived in the previous sections. To simplify notation, we consider a smooth concave boundary. More general boundaries can be treated similarly.

Let $c(s)$ be a concave and differentiable function on $[0, t]$. For any $n > 1$, let $T_n = (t_i)_0^n$ be the set of partition points of $[0, t]$ such that $0 = t_0 < t_1 < \cdots < t_{n-1} < t_n = t$. In addition, suppose T_n is a sequence of monotone increasing sets in the sense that $T_n \subset T_{n+1}$ for every n and $\lim_{n\to\infty} \max_{1\le i\le n}(t_i - t_{i-1}) = 0$. Let $b_n(s)$ be the polygonal function connecting the knots $(t_i, c(t_i)), i = 0, 1, \cdots, n$. Then it is clear that $b_n(s)$ converges to $c(s)$ uniformly on $[0, t]$ as $n \to \infty$. Therefore if $A_n = \{W_s < b_n(s), 0 \le s \le t\}$ and $A = \{W_s < c(s), 0 \le s \le t\}$, then $A_n \subset A_{n+1}$ and $\bigcup_{n=1}^{\infty} A_n = A$. It follows from the
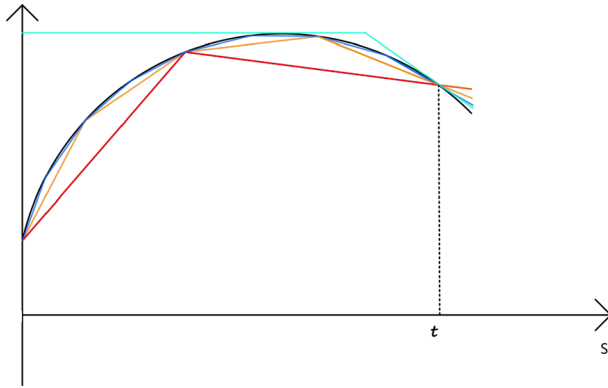
Fig. 3 Increasing piecewise linear boundaries approximating a concave boundary

continuity property of the probability measure that $\lim_{n\to\infty} P(A_n) = P(A)$. Thus we have the following result.

Theorem 6 *Let $c(s)$ be concave and differentiable on $[0, t]$ and $b_n(s)$ be the polygonal function connecting the knots (t_i, c_i), $i = 0, 1, \cdots, n$. Then $\lim_{n\to\infty} P(t; b_n) = P(t; c)$.*

Unfortunately the corresponding result for the FPD cannot be obtained in this way. To deal with the density, we construct two sequences of monotone boundaries approaching $c(s)$ from above and below respectively. Specifically, let $b_n(s)$ be defined as before. Then, since $c(s)$ is concave, $b_{n+1}(s)$ is above $b_n(s)$ for every n. It follows from Corollary 5 that $f(t; b_n) < f(t; b_{n+1})$. Further, we can always define a piecewise linear boundary $b(s)$ that is above $c(s)$ and such that $b(t) = b_n(t)$ for all n (the green boundary in Fig. 3). Then again by Corollary 5 we have $f(t; b_n) < f(t; b)$ for all n. It follows that $f(t; b_n)$ is monotone increasing and bounded from above. Therefore $\lim_{n\to\infty} f(t; b_n)$ exists and is finite.

Further, let $a_n(s)$ be the piecewise linear function consisting of the tangent lines at (t_i, c_i) (the green boundary in Fig. 4). Then it is easy to see that $a_n(s)$ is decreasing and converges
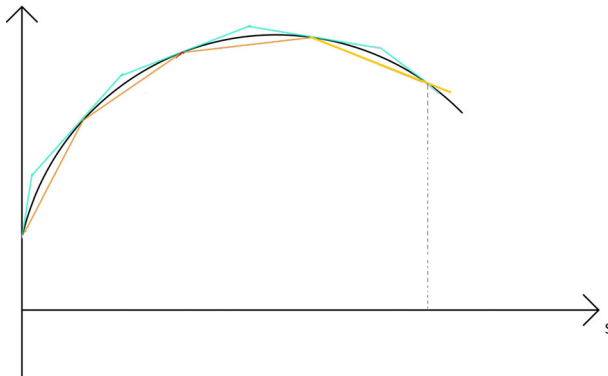

Fig. 4 Two piecewise linear boundaries approximating a concave boundary

uniformly to $c(s)$ from above, which implies that the corresponding FPD $f(t; a_n)$ is monotone decreasing and bounded from below, and therefore $\lim_{n\to\infty} f(t; a_n)$ exists. Finally, it is obvious that $f(t; b_n) \leq f(t; a_n)$ for any n. Thus we have the following results.

Theorem 7 *Let $c(s)$ be concave and differentiable on $[0, t]$, $b_n(s)$ be the piecewise linear function connecting the knots (t_i, c_i), $i = 0, 1, \cdots, n$, and $a_n(s)$ be the piecewise linear function consisting of the tangent lines to $c(s)$ at $t_i, i = 0, 1, \cdots, n$. Then their corresponding FPDs have the following properties: (1) $f(t; b_n)$ is monotone increasing and $\lim_{n\to\infty} f(t; b_n)$ exists; (2) $f(t; a_n)$ is monotone decreasing and $\lim_{n\to\infty} f(t; a_n)$ exists; and (3) $\lim_{n\to\infty} f(t; b_n) \leq \lim_{n\to\infty} f(t; a_n)$.*

5 Other Diffusion Processes

The formulas of Sections 2 and 3 can be used to obtain explicit formulas for the BCP and FPD of more general diffusion processes that can be expressed as functionals of standard Brownian motion. Such processes include geometric Brownian motion, Ornstein-Uhlenbeck processes and growth processes (Wang and Pötzelberger 2007).

Let $X = \{X_t, t \geq 0, X_0 = x_0\}$ be a diffusion process defined on a probability space $(\Omega, \mathcal{A}, P)$ with state space either the real space $\mathbb{R}$ or a subinterval of it. Denote the BNCP of X over boundary $c(s)$ on interval $[0, t]$ by

$$P_X(t; c) = P(X_s < c(s), 0 < s \leq t)$$

and the corresponding FPD by

$$f_X(t; c) = -\frac{\partial P_X(t; c)}{\partial t}.$$

Example 2 (Brownian motion with drift) It is well-known that a Brownian motion with time dependent drift can be written as $X_t = \sigma W_t + \mu(t)t$, where W_t is the standard Brownian motion. Then the BCP for X crossing the boundary $c(s)$ is given by

$$P_X(t; c) = P_W(t; d), \quad d(s) = \frac{c(s) - \mu(s)s}{\sigma}.$$

Therefore the corresponding FPD is given by $f_X(t; c) = f_W(t; d)$.

Example 3 (Ornstein-Uhlenbeck processes) An Ornstein-Uhlenbeck (OU) process is defined in state space $\mathbb{R}$ and satisfies the stochastic differential equation

$$dX_t = \kappa(\alpha - X_t)dt + \sigma dW_t, \quad X_0 = x_0,$$

where $\kappa, \sigma \in \mathbb{R}_+$ and $\alpha \in \mathbb{R}$ are constants. Then by Wang and Pötzelberger (2007) the BCP for X is given by $P_X(t; c) = P_W(T; d)$, where $T = \sigma^2(e^{2\kappa t} - 1)/2\kappa$,

$$d(s) = \alpha - x_0 + [c(g(s)) - \alpha]\left(1 + \frac{2\kappa s}{\sigma^2}\right)^{1/2},$$

and

$$g(s) = \frac{1}{2\kappa}\log\left(1 + \frac{2\kappa s}{\sigma^2}\right), s \geq 0.$$

Therefore the FPD is given by $f_X(t; c) = \sigma^2 e^{2\kappa t} f_W(T; d)$. In particular, consider a special case where $c(s) = h > 0, \alpha = x_0, \sigma^2 = 2\kappa = 1$ and $h = x_0 + 1$. Then $d(s) = \sqrt{1+s}$ for $0 \leq s \leq T = e^t - 1$. Therefore $P_X(t; h) = P_W(T; d)$ and $f_X(t; h) = e^t f_W(T; d)$.

6 Numerical Computation and Examples

Numerical computation of the BCP and FPD formulas of the previous sections is straightforward by using the Monte Carlo integration method. For example, since the BNCP $P(t; c)$ in Eq. 6 is the mathematical expectation with respect to the Gaussian random vector $W = (W_{t_1}, W_{t_2}, \cdots, W_{t_n})$, a natural estimator is $P_m = \sum_{j=1}^{m} g_n(\mathbf{w}_n^j; c)/m$, where $\mathbf{w}_j = (w_{j1}, w_{j2}, \ldots, w_{jn})$, $j = 1, 2, \ldots, m$, are independent random vectors generated from the multivariate Gaussian distribution of W. Then the strong law of large numbers guarantees $P_m \to P(t; c)$ almost surely as $m \to \infty$, and the central limit theorem implies that $P_m - P(t; c) = O_p(m^{-1/2})$. Furthermore, the simulation precision can be assessed by the corresponding simulation standard error

$$se = [\sum_{j=1}^{m} (g_n(\mathbf{w}_j) - P_m)^2 / m(m-1)]^{1/2}.$$

Therefore the approximation error can be reduced by increasing the simulation size m.

For continuous piecewise linear boundaries, the calculation using the alternative formula (8) is even simpler because the random vectors $\mathbf{w}_j = (w_{j1}, w_{j2}, \ldots, w_{jn})$ can be directly generated from the distribution of $(W_{t_1} - c_1, W_{t_2} - c_2, \cdots, W_{t_n} - c_n)$, so that the integrant $g_n(\mathbf{w}_j)$ does not involve boundary points $(c_1, c_2, \ldots, c_n)$ at all. The FPD can be calculated similarly.

In the following we calculate some examples to further demonstrate this method. In all examples, we use simulation sample size $m = 2 \times 10^5$ except the results in Table 1, which uses $m = 2 \times 10^6$. The numerical calculations are done using the MATLAB on a 64-bit Windows workstation with a 3.60GHz Intel CPU and 16GB RAM.

Example 4 (BCP for Daniels' boundary) The Daniels' boundary (Daniels 1996) is widely used in the literature as a benchmark example for testing numerical methods for BCP and FPD since the exact results are known. It is defined as

$$c(s) = \frac{1}{2} - s \log \left(\frac{1}{4} + \frac{1}{4}\sqrt{1 + 8 \exp(-\frac{1}{s})} \right), s \geq 0.$$

For $t = 1$, the exact result is known to be $P(t; c) = 0.520251$. By using 64 partition points, we obtain an estimate $P_m = 0.520206$ with simulation standard error $se = 0.001086$ and computation time 0.993175 seconds. In order to see how the approximation accuracy improves with the increase of partition size n, we calculate the $P(t; c)$ again for various n with simulation size $m = 2 \times 10^6$. The results in Table 1 show clearly that when n increases the approximation becomes more and more accurate and stable. Note that the standard errors do not change with n.

Table 1 The BNCP $P(t; c)$, $t = 1$ for Daniels' boundary with various n. The simulation standard errors are in parentheses

$n = 2$	$n = 4$	$n = 6$	$n = 8$	$n = 10$	$n = 12$	$n = 14$
0.506537	0.518079	0.519547	0.519367	0.520332	0.520601	0.519925
(0.000282)	(0.000309)	(0.000319)	(0.000324)	(0.000328)	(0.000330)	(0.000332)
$n = 16$	$n = 20$	$n = 26$	$n = 32$	$n = 64$	$n = 128$	Exact
0.520183	0.520482	0.520777	0.520178	0.520454	0.520310	0.520251
(0.000334)	(0.000336)	(0.000338)	(0.000339)	(0.000347)	(0.000346)	

Table 2 The BCP $P(t;c), t = 1$ for some nonlinear boundaries using various partition sizes. Simulation standard errors are in parentheses

$c(s)$	$n = 4$	$n = 8$	$n = 16$	$n = 32$	$n = 64$
$\sqrt{1+s}$	0.804894	0.804740	0.802533	0.804751	0.804485
	(0.000799)	(0.000826)	(0.000849)	(0.000858)	(0.000867)
$0.5\sqrt{1+s}$	0.450516	0.450433	0.452872	0.449928	0.450653
	(0.000971)	(0.001019)	(0.001050)	(0.001068)	(0.001081)
$\exp(-s)$	0.439668	0.437573	0.436956	0.438864	0.439186
	(0.001047)	(0.001019)	(0.001065)	(0.001079)	(0.001088)
$1 + s^2$	0.856445	0.852497	0.851839	0.853728	0.852372
	(0.000689)	(0.000728)	(0.000748)	(0.000759)	(0.000771)
$1 + s - s^2$	0.740651	0.741056	0.743063	0.744337	0.744190
	(0.000903)	(0.000925)	(0.000939)	(0.000949)	(0.000957)

Example 5 Now we calculate the BCP for some nonlinear boundaries which have been used before by Wang and Pötzelberger (Wang and Pötzelberger 1997) and some other authors. The numerical results are given in Table 2, which are in line with the results obtained previously in the literature.

Table 3 Exact and estimated FPD with various n for square-root boundary $\sqrt{1+s}$

t	Exact	$n = 16$	$n = 32$	$n = 64$	$n = 128$
0.2	0.2234	0.2227	0.2223	0.2230	0.2229
0.3	0.2810	0.2803	0.2799	0.2794	0.2806
0.4	0.2772	0.2772	0.2771	0.2762	0.2782
0.5	0.2559	0.2558	0.2555	0.2552	0.2561
0.6	0.2311	0.2308	0.2315	0.2318	0.2316
0.7	0.2081	0.2076	0.2070	0.2082	0.2076
0.8	0.1871	0.1867	0.1869	0.1864	0.1868
0.9	0.1685	0.1686	0.1683	0.1688	0.1690
1.0	0.1529	0.1532	0.1532	0.1524	0.1539
1.2	0.1278	0.1276	0.1277	0.1280	0.1279
1.4	0.1089	0.1089	0.1091	0.1091	0.1091
1.6	0.0946	0.0941	0.0947	0.0942	0.0944
1.8	0.0827	0.0824	0.0827	0.0827	0.0822
2.0	0.0732	0.0732	0.0732	0.0731	0.0732
2.5	0.0564	0.0564	0.0565	0.0565	0.0562
3.0	0.0455	0.0453	0.0454	0.0455	0.0452
3.5	0.0376	0.0377	0.0377	0.0375	0.0379
4.0	0.0320	0.0320	0.0320	0.0321	0.0319
4.5	0.0277	0.0277	0.0278	0.0277	0.0278
5.0	0.0243	0.0243	0.0243	0.0244	0.0244
5.5	0.0216	0.0216	0.0217	0.0216	0.0216
6.0	0.0195	0.0194	0.0194	0.0195	0.0194

Table 4 Exact and estimated FPD with various n for boundary $0.5\sqrt{1+s}$

| t	Exact	$n = 16$	$n = 32$	$n = 64$	$n = 128$
0.05	1.2871	1.2926	1.2926	1.2890	1.2854
0.1	1.5976	1.5954	1.5954	1.5971	1.5972
0.15	1.3181	1.3173	1.3185	1.3201	1.3187
0.2	1.0570	1.0561	1.0548	1.0603	1.0568
0.25	0.8592	0.8576	0.8585	0.8556	0.8588
0.3	0.7085	0.7107	0.7087	0.7104	0.7100
0.35	0.5978	0.5996	0.5987	0.5997	0.5988
0.4	0.5137	0.5151	0.5141	0.5133	0.5140
0.45	0.4461	0.4452	0.4458	0.4465	0.4463
0.5	0.3924	0.3929	0.3929	0.3918	0.3921
0.6	0.3122	0.3120	0.3116	0.3123	0.3118
0.7	0.2568	0.2563	0.2559	0.2563	0.2563
0.8	0.2152	0.2151	0.2153	0.2140	0.2153
0.9	0.1837	0.1842	0.1843	0.1837	0.1838
1.0	0.1598	0.1597	0.1599	0.1593	0.1599
1.2	0.1253	0.1252	0.1252	0.1247	0.1252
1.4	0.1012	0.1017	0.1015	0.1023	0.1019
1.6	0.0848	0.0846	0.0844	0.0846	0.0847
1.8	0.0720	0.0719	0.0719	0.0721	0.0721
2.0	0.0621	0.0621	0.0623	0.0621	0.0622
2.2	0.0545	0.0546	0.0547	0.0542	0.0544
2.4	0.0485	0.0483	0.0484	0.0483	0.0484
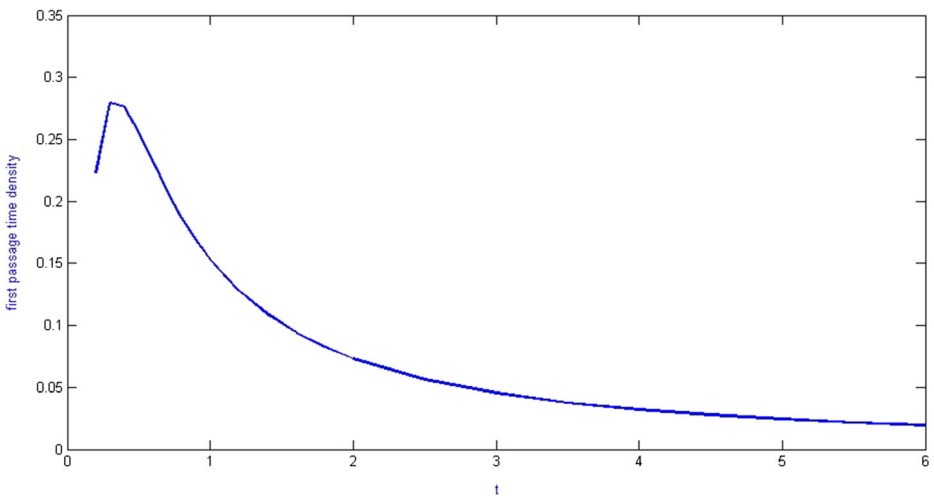
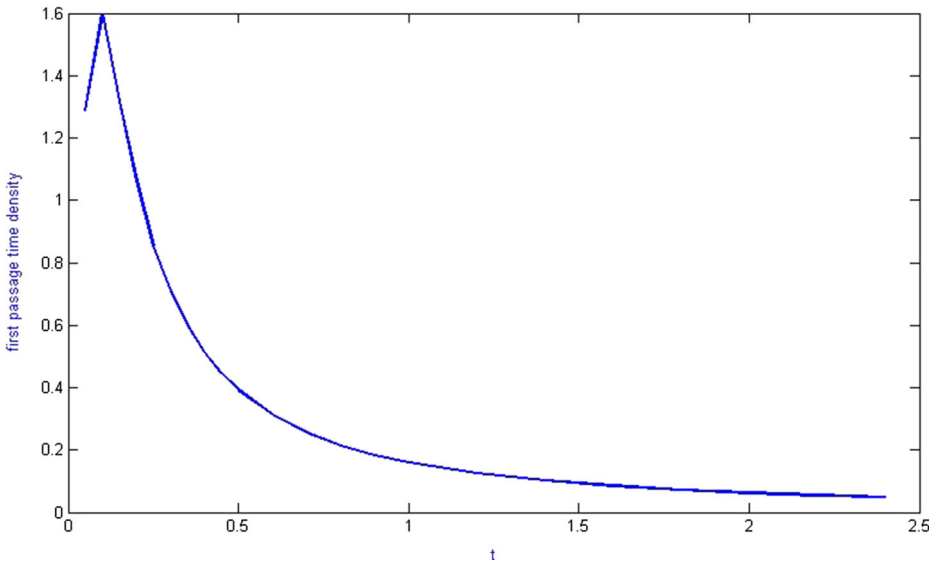**Fig. 5** Exact and estimated FPD with $n = 64$ for boundary $\sqrt{1+s}$

Fig. 6 Exact and estimated FPD with $n = 64$ for boundary $0.5\sqrt{1+s}$

Example 6 (FPD for square-root boundary) Square-root boundary is another benchmark example that is widely used in the literature to test various numerical algorithms. We also calculate the FPD for two such boundaries with various partition sizes and the results are given in Tables 3 and 4, where the exact values are taken from (Daniels 1996). These results show that our method provides fairly good estimates. The exact and estimated FPD with $n = 64$ are also plotted in Figs. 5 and 6. The two curves are too close to be distinguishable.

Example 7 (FPD for nonlinear boundaries) Now we calculate the FPD for some nonlinear boundaries $c(s) = 1+s^2$, $c(s) = 1+s-s^2$ and $c(s) = \exp(-s)$. The numerical results with partition size $n = 64$ are respectively shown in Tables 5, 6 and 7, while their corresponding line plots are shown in Figs. 7, 8 and 9.

Table 5 The approximated FPD with $n = 64$ for boundary $1 + s^2$

t	0.05	0.10	0.15	0.20	0.25	0.30	0.35	0.40
FPD	0.0008	0.0763	0.2067	0.2941	0.3148	0.3102	0.2902	0.2583
	0.45	0.5	0.55	0.60	0.65	0.70	0.75	0.80
	0.2231	0.1932	0.1663	0.1400	0.1133	0.0956	0.0788	0.0633
	0.85	0.9	0.95	1.0	1.1	1.2	1.3	1.4
	0.0507	0.0409	0.0328	0.0255	0.0254	0.0149	0.0086	0.0049

Table 6 The approximated FPD with $n = 64$ for boundary $1 + s - s^2$

t	0.05	0.10	0.15	0.20	0.25	0.30	0.35	0.40
FPD	0.0002	0.0317	0.1012	0.1547	0.1968	0.2267	0.2492	0.2613
	0.45	0.5	0.55	0.60	0.65	0.70	0.75	0.80
	0.2742	0.2821	0.2928	0.3024	0.3151	0.3271	0.3409	0.3580
	0.85	0.9	0.95	1.0	1.1	1.2	1.3	1.4
	0.3761	0.3894	0.4097	0.4269	0.4699	0.5046	0.5472	0.5795
	1.5	1.6	1.7	1.8	1.9	2.0	2.1	2.2
	0.5989	0.6110	0.6062	0.5850	0.5456	0.4891	0.4244	0.3526
	2.3	2.4	2.5	2.6	2.7	2.8	2.9	3.0
	0.2784	0.2115	0.1489	0.1020	0.0649	0.0386	0.0223	0.0111
	3.1	3.2	3.3	3.4	3.5			
	0.0056	0.0024	0.0010	0.0004	0.0002			

Table 7 The approximated FPD with $n = 64$ for boundary $\exp(-s)$

| t	0.05	0.10	0.15	0.20	0.25	0.30	0.35	0.40
FPD	0.0045	0.2074	0.5931	0.8312	0.9206	0.9334	0.9084	0.8632
	0.45	0.5	0.55	0.60	0.65	0.70	0.75	0.80
	0.7917	0.7289	0.6668	0.6098	0.5529	0.5055	0.4673	0.4283
	0.85	0.9	0.95	1.0	1.1	1.2	1.3	1.4
	0.3904	0.3597	0.3298	0.3063	0.2637	0.2304	0.1994	0.1743
	1.5	1.6	1.7	1.8	1.9	2.0	2.1	2.2
	0.0596	0.0571	0.0525	0.0483	0.0462	0.0434	0.0870	0.0759
	2.3	2.4	2.5	2.6	2.7	2.8	2.9	3.0
	0.0702	0.0655	0.0596	0.0571	0.0525	0.0483	0.0462	0.0434
	3.1	3.2	3.3	3.4	3.5			
	0.0406	0.0385	0.0361	0.0344	0.0324			
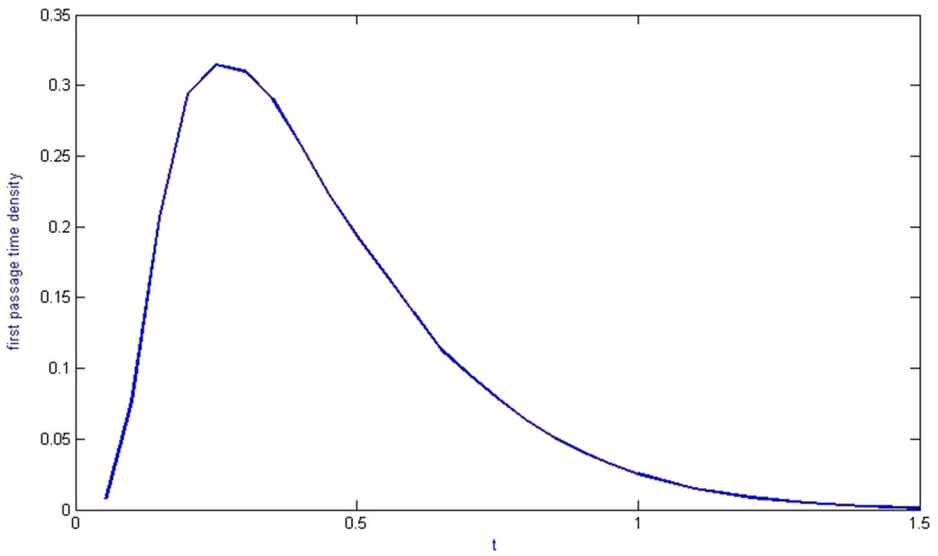
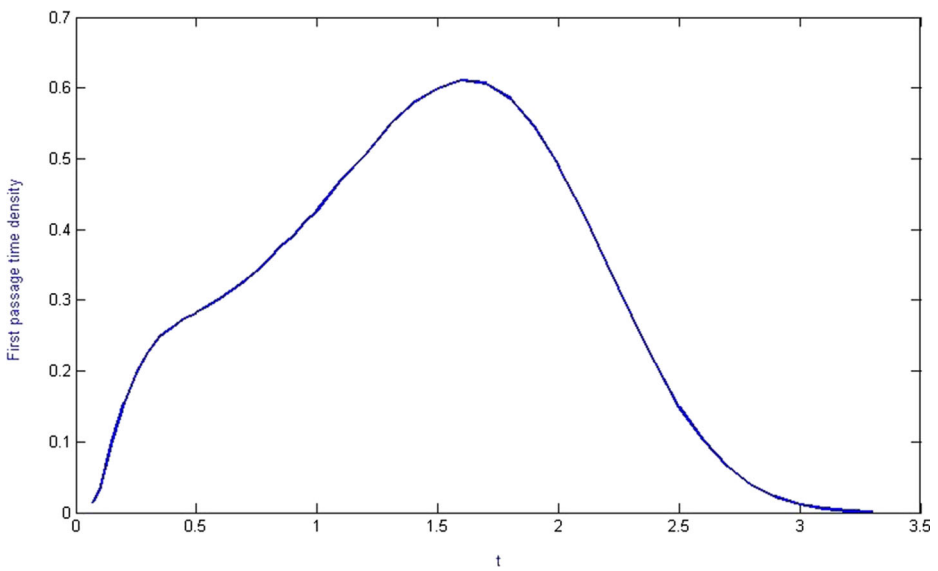**Fig. 7** The approximated FPD with $n = 64$ for boundary $1 + s^2$

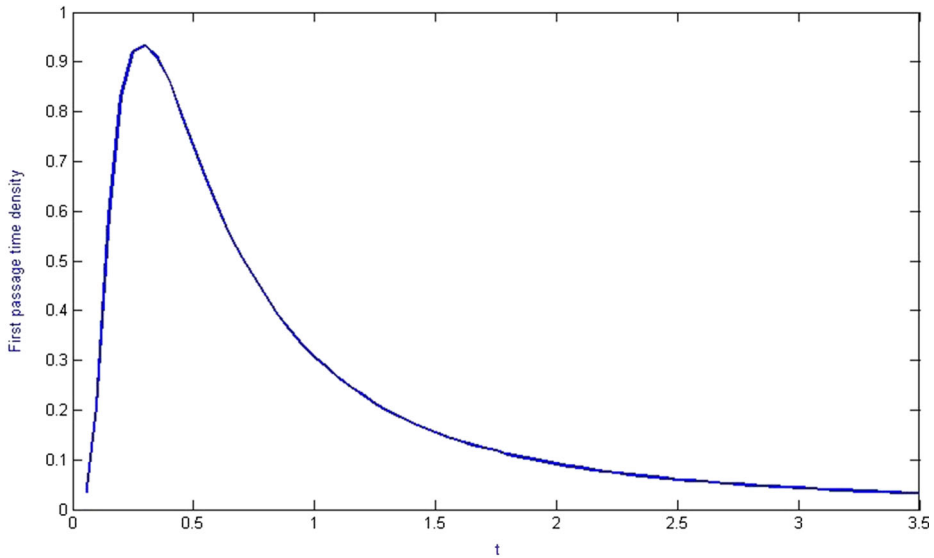**Fig. 8** The approximated FPD with $n = 64$ for boundary $1 + s - s^2$

Fig. 9 The approximated FPD with $n = 64$ for boundary $\exp(-s)$

7 Conclusions and Discussion

The calculation of boundary crossing probabilities and first passage time densities are important but challenging problems. The main stream approaches are based on certain differential or integral equations and deal with smooth boundaries only. We proposed an approach that apply to smooth as well as discontinuous boundaries. Using this approach we have derived explicit formulas for the piecewise linear boundary crossing probability and density for Brownian motion. The derived formulas can be used to approximate the BCP or FPD for more general nonlinear boundaries.

We have demonstrated that the numerical calculation can be easily done by Monte Carlo simulation method and the simulation error can be easily assessed. We have tested our method on some well-known benchmark examples and our numerical results show that this method produces fairly good approximations.

We have also shown how to obtain closed-form BCP or FPD for a class of diffusion processes that can be expressed as piecewise monotone functionals of Brownian motion, including geometric Brownian motion, O-U processes and growth processes. Moreover, this method can be extended to two-sided boundary crossing problems.

References

Buonocore A, Nobile AG, Ricciardi LM (1987) A new integral equation for the evaluation of first-passage-time probability densities. Adv Appl Probab:784–800
Daniels HE (1982) Sequential tests constructed from images. Ann Stat 10:394–400

Daniels HE (1996) Approximating the first crossing-time density for a curved boundary. Bernoulli 2:133–143

Durbin J (1971) Boundary crossing probabilities for the Brownian motion and Poisson processes and techniques for computing the power of the Kolmogorov-Smirnov test. J Appl Probab 8:431–453

Durbin J, Williams D (1992) The first-passage density of the Brownian motion process to a curved boundary. J Appl Probab 29:291–304

Ferebee B (1982) The tangent approximation to one-sided Brownian exit densities. Zeitschrift für Wahrscheinlichkeitstheorie und Verwandte Gebiete 61:309–326

Ferebee B. (1983) An asymptotic expansion for one-sided Brownian exit densities. Probab Theory Relat Fields 63:1–15

Karatzas I, Shreve SE (1991) Brownian motion and stochastic calculus, 2nd edn. Springer, New York

Lehmann A (2002) Smoothness of first passage time distributions and a new integral equation for the first passage time density of continuous Markov processes. Adv Appl Probab 34:869–887

Lerche HR (1986) Boundary crossing of brownian motion. Lecture notes in statistics, vol 40. Springer, Heidelberg

Molini A, Talkner P, Katul GG, Porporato A (2011) First passage time statistics of Brownian motion with purely time dependent drift and diffusion. Physica A: Statistical Mechanics and its Applications 390:1841–1852

Ricciardi LM, Sacerdote L, Sato S (1984) On an integral equation for first-passage-time probability densities. J Appl Probab 21:302–314

Siegmund D (1986) Boundary crossing probabilities and statistical applications. Ann Stat 14:361–404

Strassen V (1967) Almost sure behaviour of sums of independent random variables and martingales. Math Statist Prob 2:315–343

Taillefumier T, Magnasco MO (2010) A fast algorithm for the first-passage times of Gauss-Markov processes with Hölder continuous boundaries. J Stat Phys 140:1130–1156

Wang L, Pötzelberger K (1997) Boundary crossing probability for brownian motion and general boundaries. J Appl Probab 34:54–65

Wang L, Pötzelberger K (2007) Crossing probability for some diffusion processes with piecewise continuous boundaries. Methodol Comput Appl Probab 9:21–40